Electronic Supplementary Material (ESI) for Soft Matter.
This journal is © The Royal Society of Chemistry 2016

Electronic Supplementary Information for: Elucidating the Mechanisms of Nanodiamond-Promoted Structural Disruption of Crystallised Lipid

Zak E. Hughes,*[a] **and Tiffany R. Walsh***[a]

[a] *Institute for Frontier Materials, Deakin University, Geelong, Australia. Fax: +61 (0)3 5227 1103; Tel: +61 (0)3 5247 9160; E-mail: zhughes@deakin.edu.au; tiffany.walsh@deakin.edu.au*

Contents

S1 Nanodiamond FF Parameter Generation

For our structural model, we used the octahedral C_{84} nanodiamond, which exposes the $\{111\}$ plane.[1] This nanoparticle was cleaved from the experimentally-determined structural model of bulk crystalline diamond. There were 64 surface carbon atoms in this nanoparticle, all of which were terminated with hydrogen atoms, generating a nanodiamond with composition $C_{84}H_{64}$.

The structure of this nanoparticle was optimised using a self-consistent charge density-functional tight-binding (SCC-DFTB) approach,[2] using the carbon-carbon, carbon-hydrogen and hydrogen-hydrogen Slater-Koster files,[2] The DFTB+ software package[3] was employed for these geometry optimisation calculations. The resulting relaxed nanoparticle structure was used as a basis for subsequent single-point energy (SPE) density-functional theory (DFT) calculations conducted using the B3LYP exchange-correlation functional[4,5] with 6-31G* basis sets, with the GAUSSIAN09 software package[6]. The resulting electronic density was analysed using a natural bond orbital (NBO) analysis,[7] to define partial atomic charges that were subsequently assigned to each atomic site in the nanoparticle.

To construct the force-field for the hydrogenated nanodiamond, we used these partial atomic charges, along with existing Lennard-Jones parameters for tetrahedrally-coordinated carbon, and alkane hydrogen, taken from the CHARMM36 force-field.[8] All bonded parameters (bond-stretching, etc) were similarly taken from the CHARMM36 force-field.

Table S1 Summary of the different of the systems simulated

Name	Temp. / K	Bilayer	No. of ND/Charge on ND	No. of SDBS	Number of runs
A^{4q1}	300	Yes	4 / 1	20	1
A^{4q2}	300	Yes	4 / 2	20	1
A^{4q4}	300	Yes	4 / 4	20	3
B^{4q0}	350	Yes	4 / 0	20	2
B^{4q1}	350	Yes	4 / 1	20	2
B^{4q2}	350	Yes	4 / 2	20	1
C^{4q2}	300	Yes	4 / 2	20	1
C^{8q2}	300	Yes	8 / 2	20	1
C^{4q4}	300	Yes	4 / 4	20	3
C^{8q4}	300	Yes	8 / 4	20	1
D^{4q0}	350	Yes	4 / 0	20	1
D^{4q1}	350	Yes	4 / 1	20	1
D^{4q2}	350	Yes	4 / 2	20	1
D^{4q4}	350	Yes	4 / 4	20	3
D^{8q4}	350	Yes	8 / 4	20	1
F^{4q1}	350	Yes	4 / 1	16	2
F^{4q2}	350	Yes	4 / 2	16	2
F^{4q4}	350	Yes	4 / 4	16	1
G^{4q0}	350	Yes	4 / 0	24	1
G^{4q1}	350	Yes	4 / 1	24	2
G^{4q2}	350	Yes	4 / 2	24	1
G^{4q4}	350	Yes	4 / 4	24	1
S^{4q0}	300	No	4 / 0	20	1
S^{4q1}	300	No	4 / 1	20	1
S^{4q2}	300	No	4 / 2	20	1
S^{4q4}	300	No	4 / 4	20	1
T^{4q0}	350	No	4 / 0	20	1
T^{4q1}	350	No	4 / 1	20	1
T^{4q2}	350	No	4 / 2	20	1
T^{4q4}	350	No	4 / 4	20	1

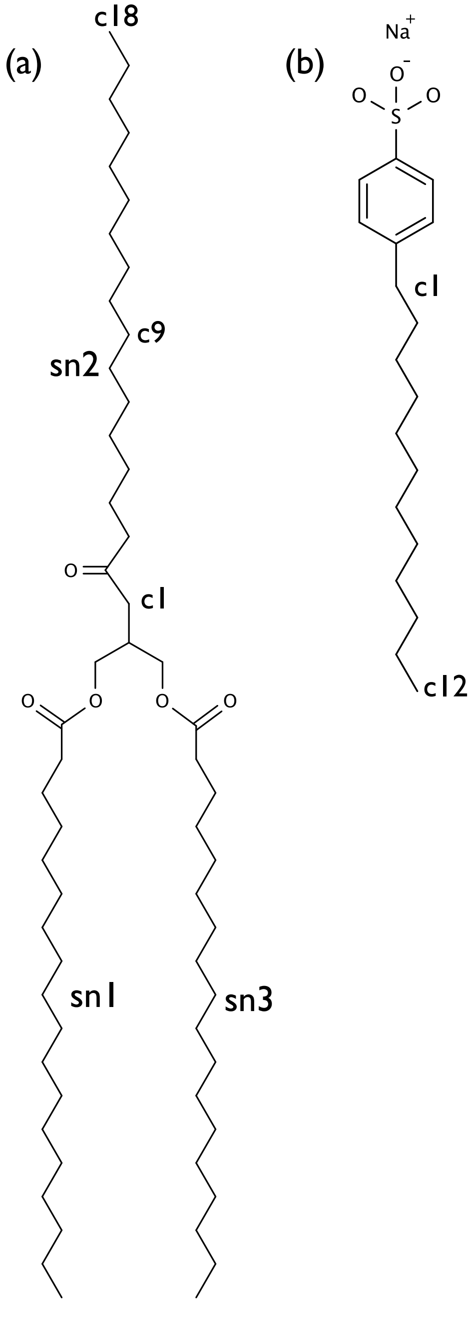

Fig. S1 The chemical structure of (a) tristearin (TS) and (b) sodium dodecylbenzene sulphonate (SDBS). The *sn*-1, *sn*-2 and *sn*-3 acyl tails of TS are marked. The C1, C9 and C18 positions in the acyl tail of TS and the C1 and C12 positions of the acyl tail of SDBS are also labelled.

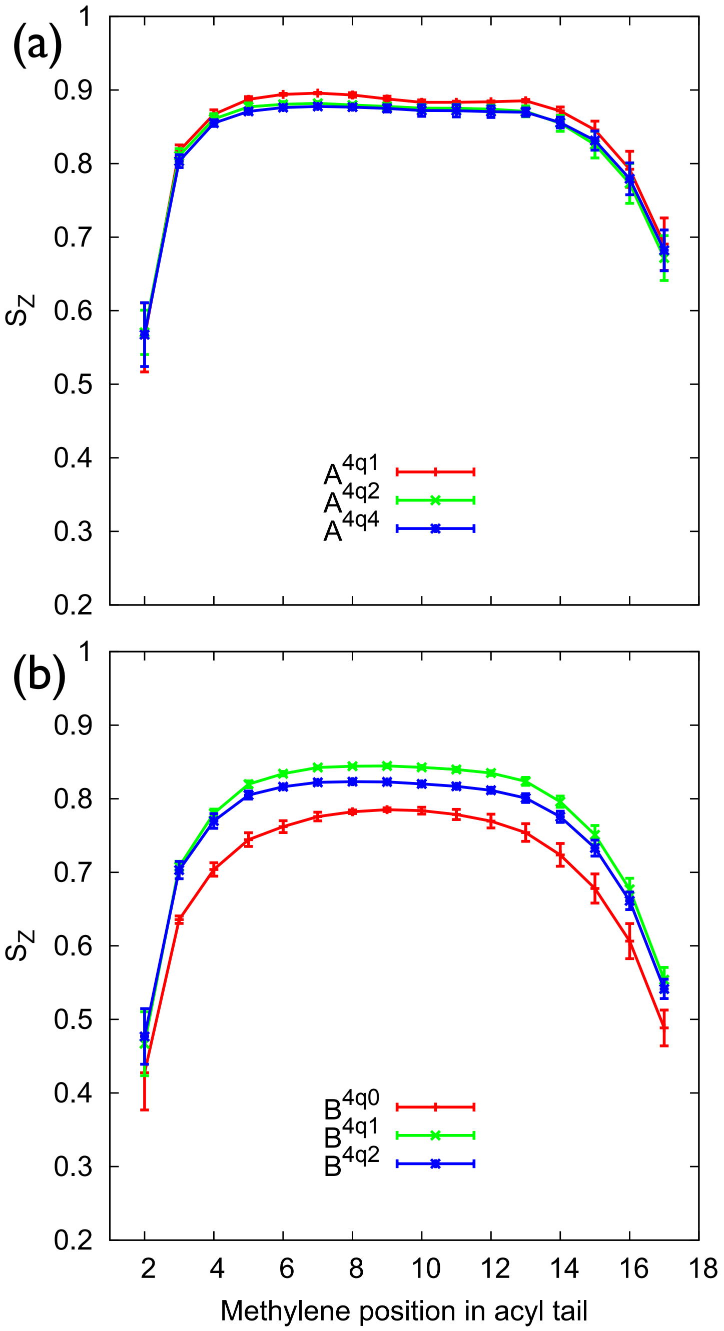

Fig. S2 Average order parameter of the acyl tails of TS molecules at 350 K for (a) Set A and (b) Set B systems.

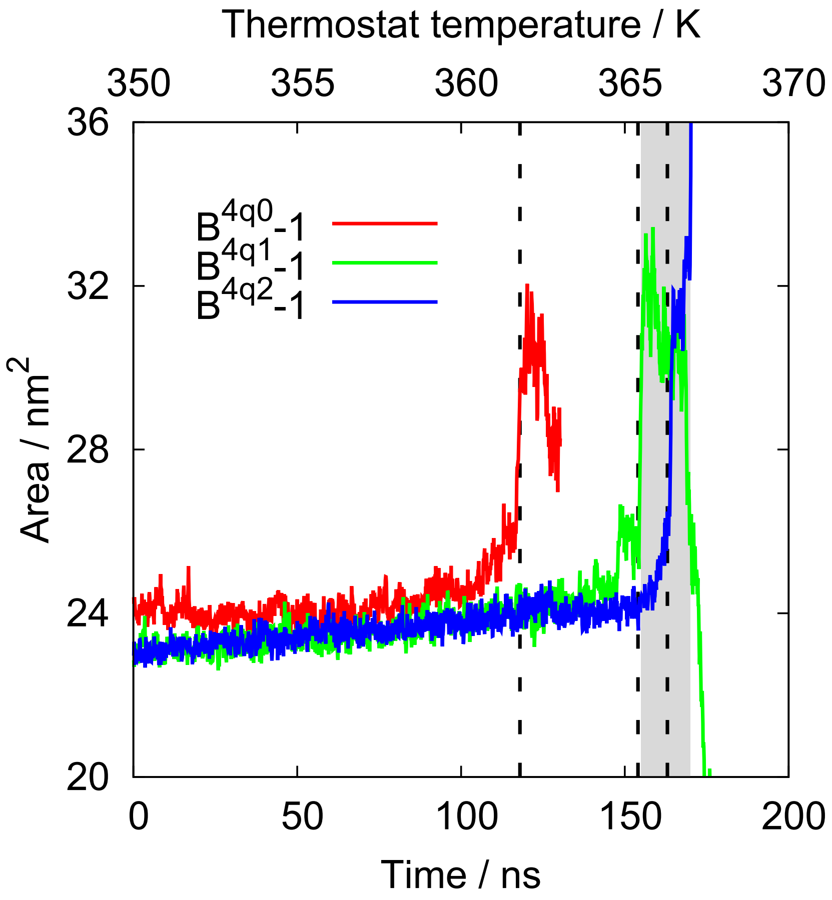

Fig. S3 Lateral area of bilayer as a function of time/temperature for the heating simulations of Set B systems. The dashed lines indicate the phase transition temperature of the different runs. The shaded area indicates the temperature range for TS bilayer in the absence of NDs.

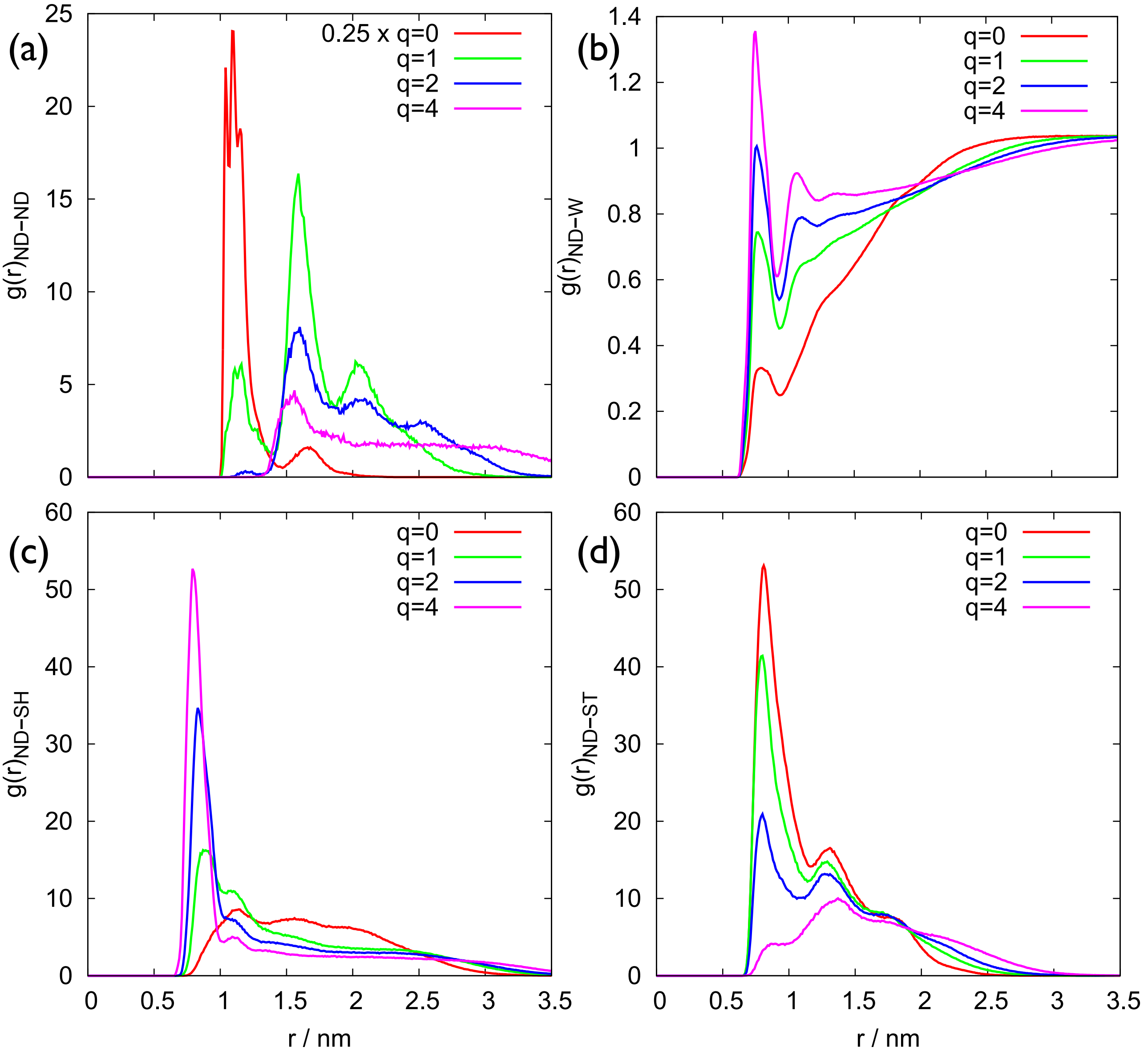

Fig. S4 Radial distribution functions of the centre of mass of molecules (a) ND-ND, (b) ND-water, (c) ND-SDBS head and (d) ND-SDBS tail.

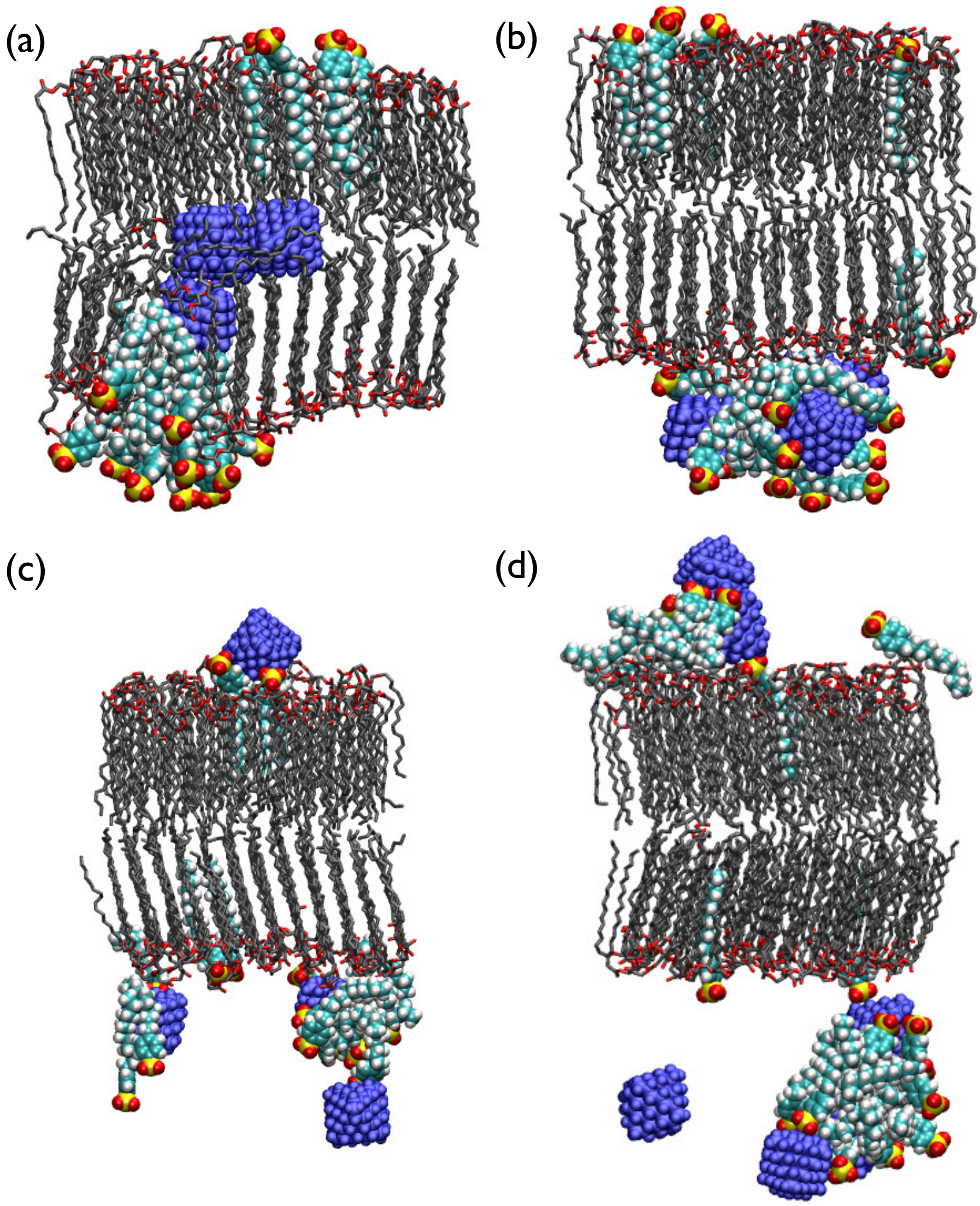

Fig. S5 Representative snapshots taken from simulations (a) D^{4q0}-1, (b) D^{4q1}-1, (c) D^{4q4}-3 and (d) D^{8q4}-1.

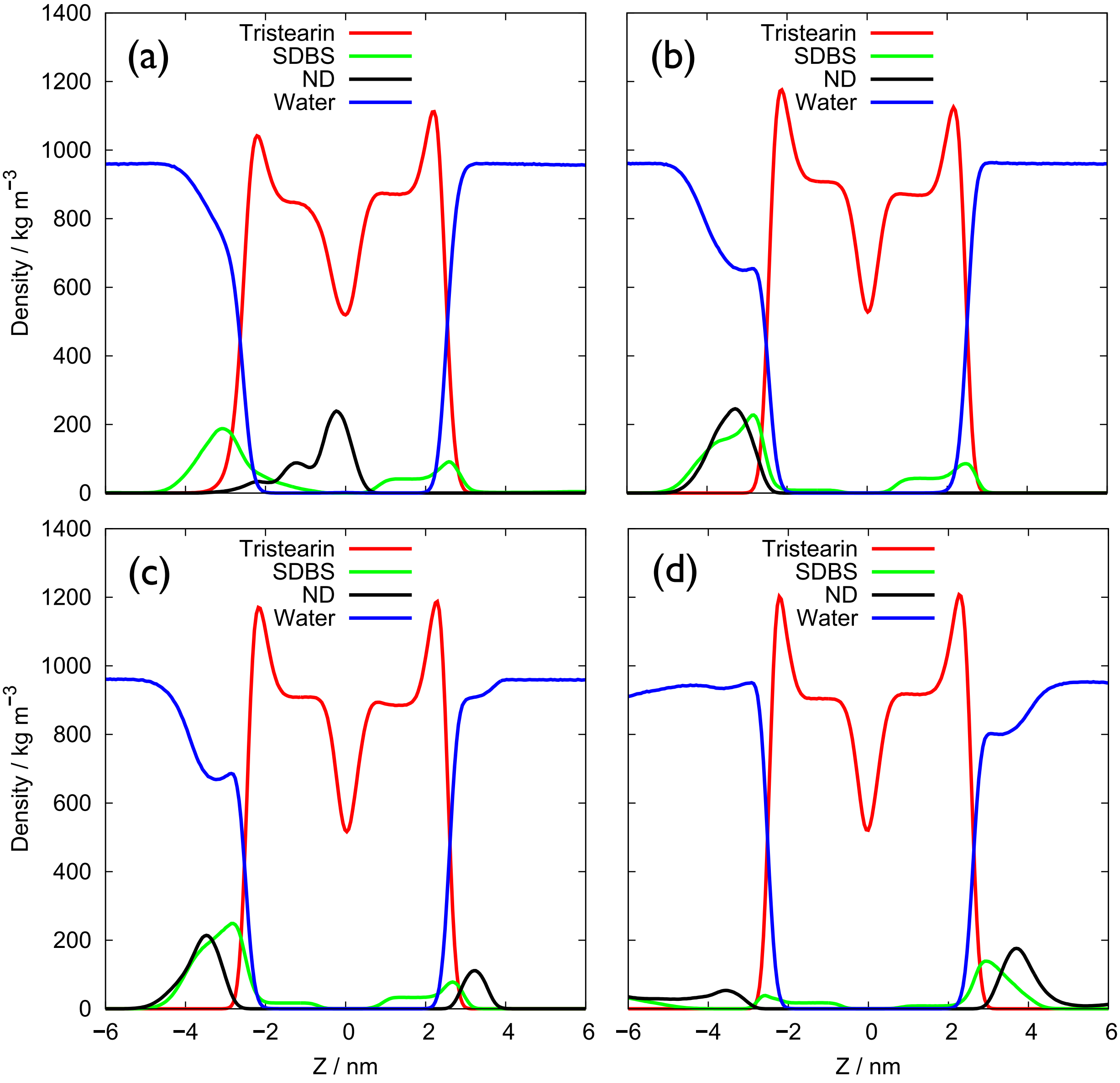

Fig. S6 Density profile of the TS bilayers from set D: (a) Run D^{4q0}-1, (b) D^{4q1}-1, (c) D^{4q4}-3 and (d) D^{8q4}-1.

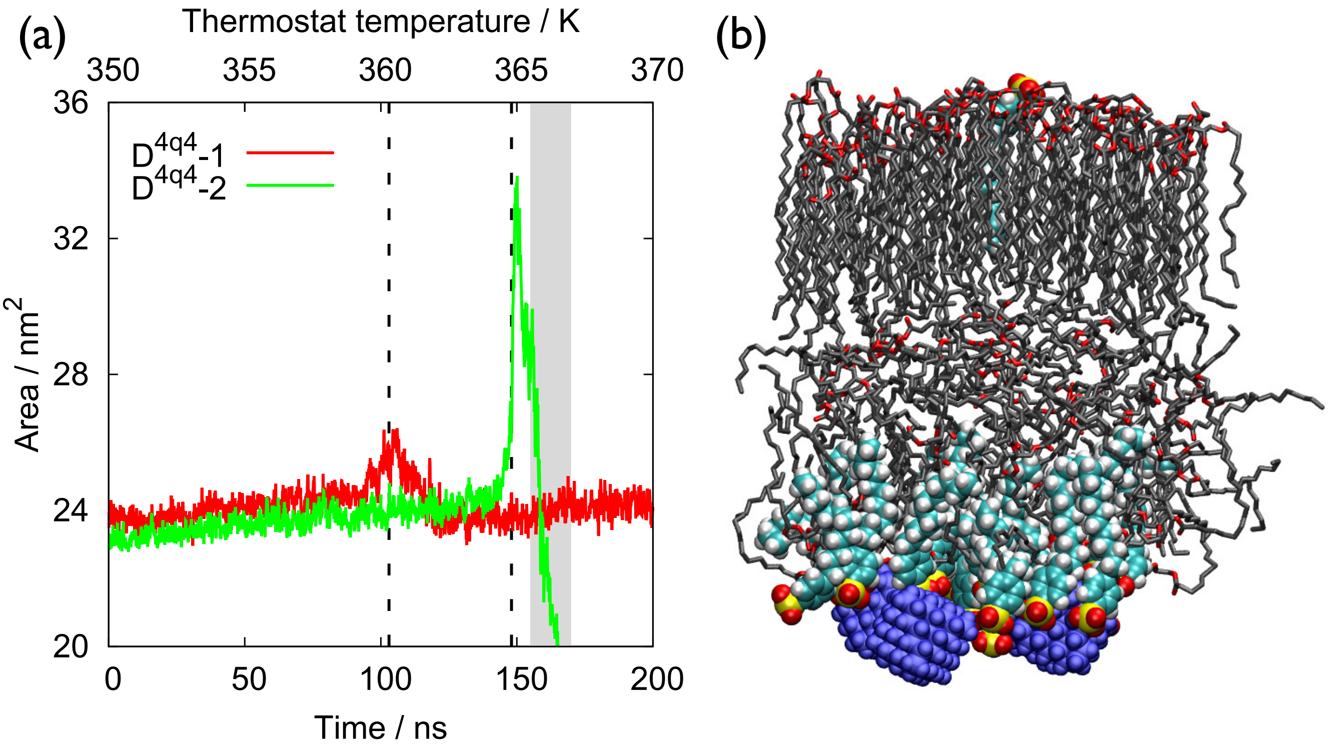

Fig. S7 (a) The area of the bilayer as a function of time/temperature during the D^{4q4} heating simulations. The vertical dashed lines indicate the transition temperature of each run. The shaded indicates the temperature range for phase transition of pure TS bilayers in the absence of NDs and SDBS. (b) a snapshot of taken from D^{4q4}-1 at 125 ns, showing the phase transition that has occurred in the lower leaflet of the bilayer

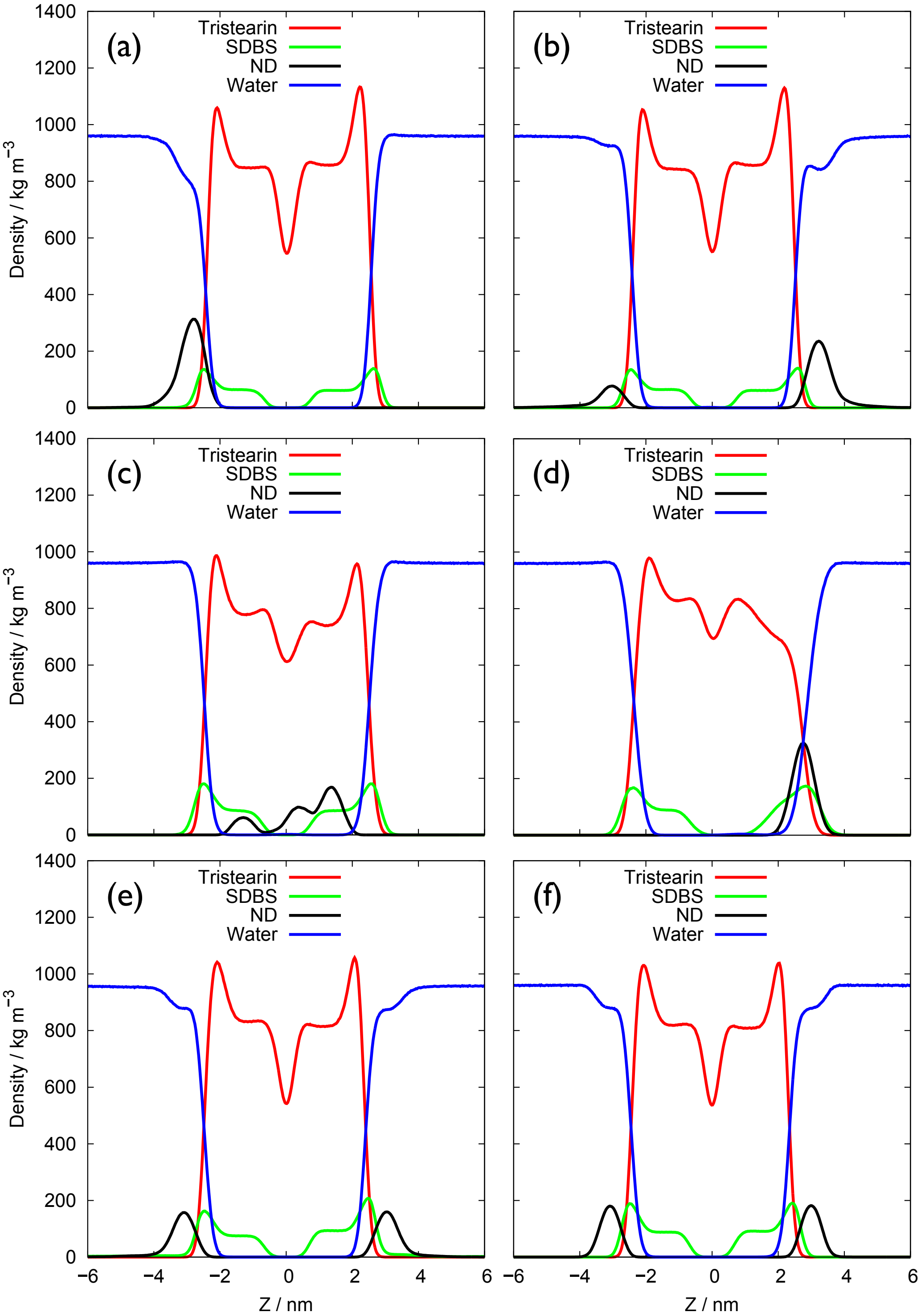

Fig. S8 Density profile of the TS bilayers from set F (a) and (b) and set G (c) to (f): (a) F^{4q1}-1, (b) F^{4q2}-1, (c) G^{4q0}-1, (d) G^{4q1}-1, (e) G^{4q2}-1 and (f) G^{4q4}-1.

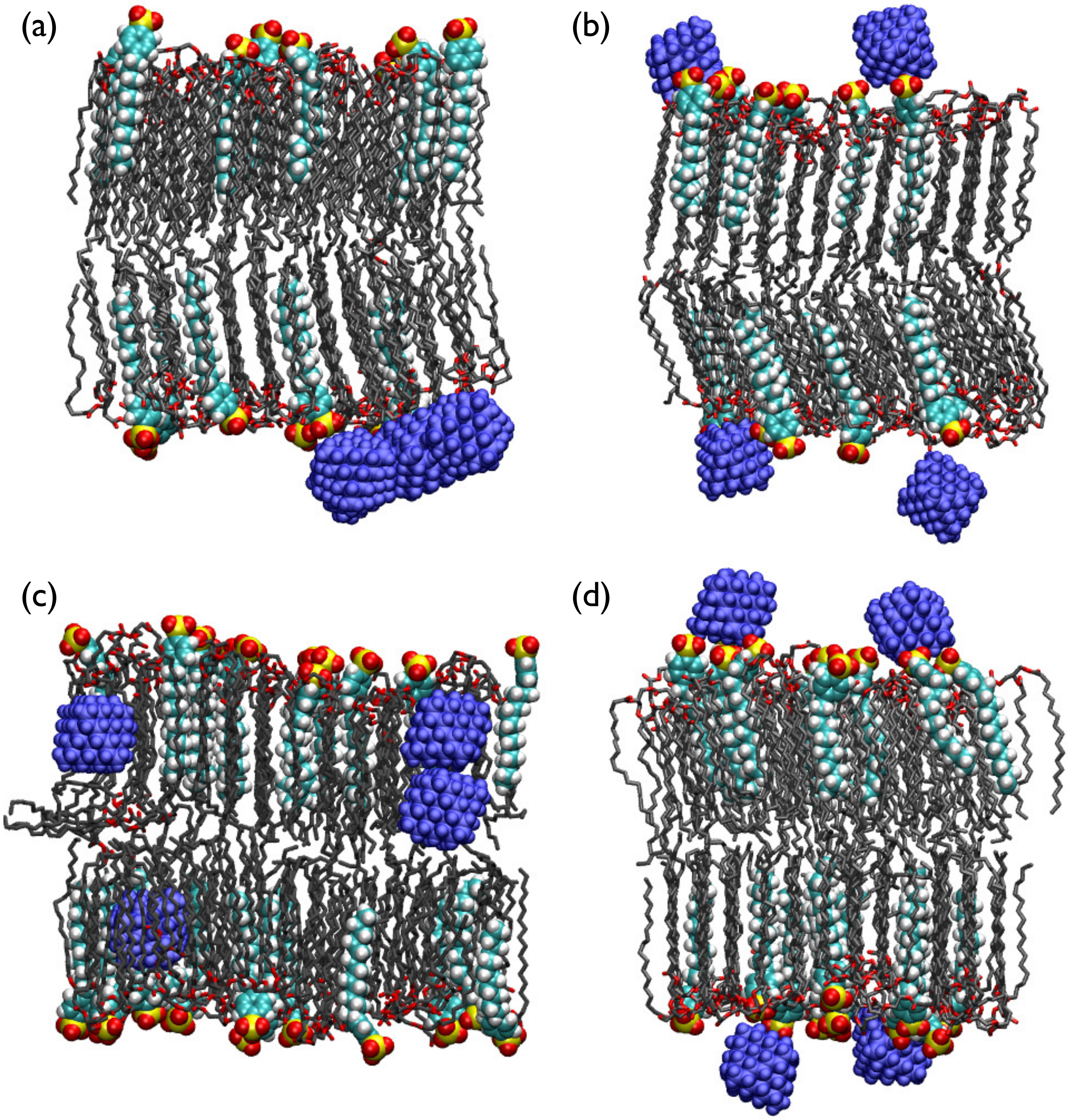

Fig. S9 Representative snapshots taken from simulations (a) F^{4q1}-1, (b) F^{4q2}-1, (c) G^{4q0}-1 and (d) G^{4q4}-1

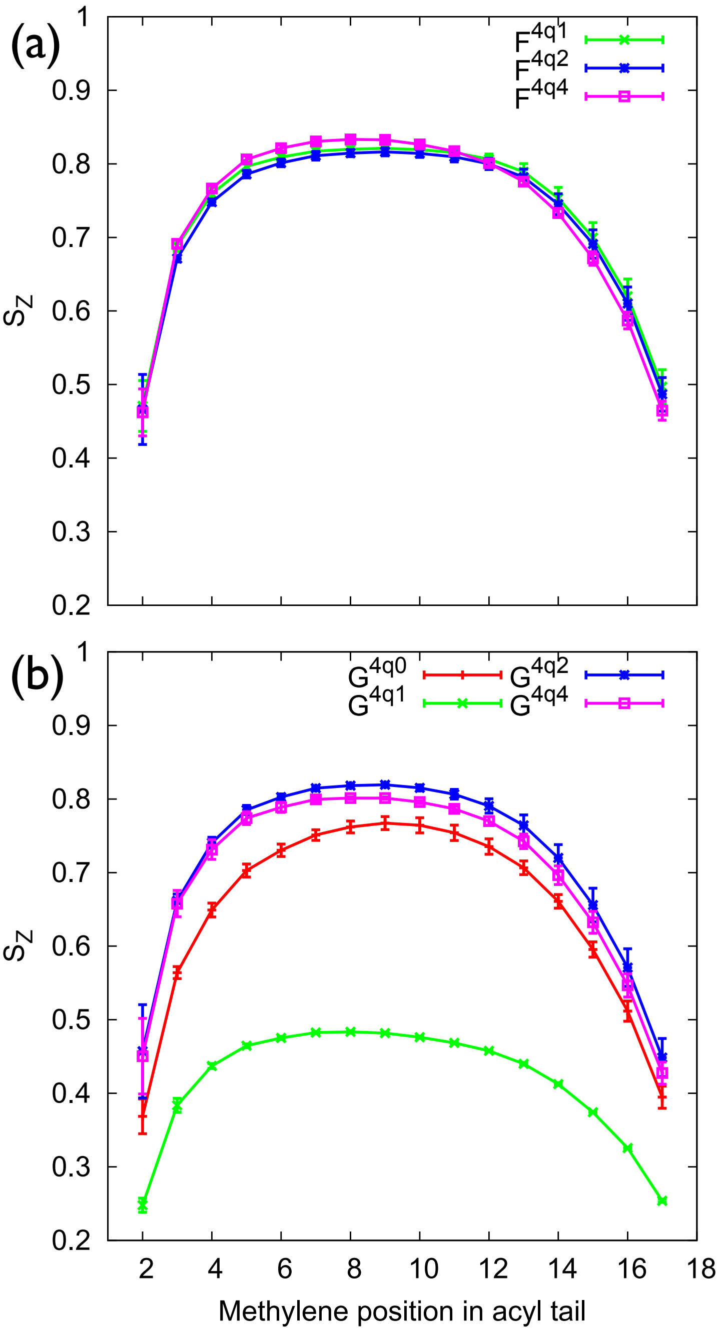

Fig. S10 Average order parameter of the acyl tails of TS molecules at 350 K in mixed TS-SDBS bilayers containing (a) 16 (Set F) and (b) 24 SDBS (Set G) molecules

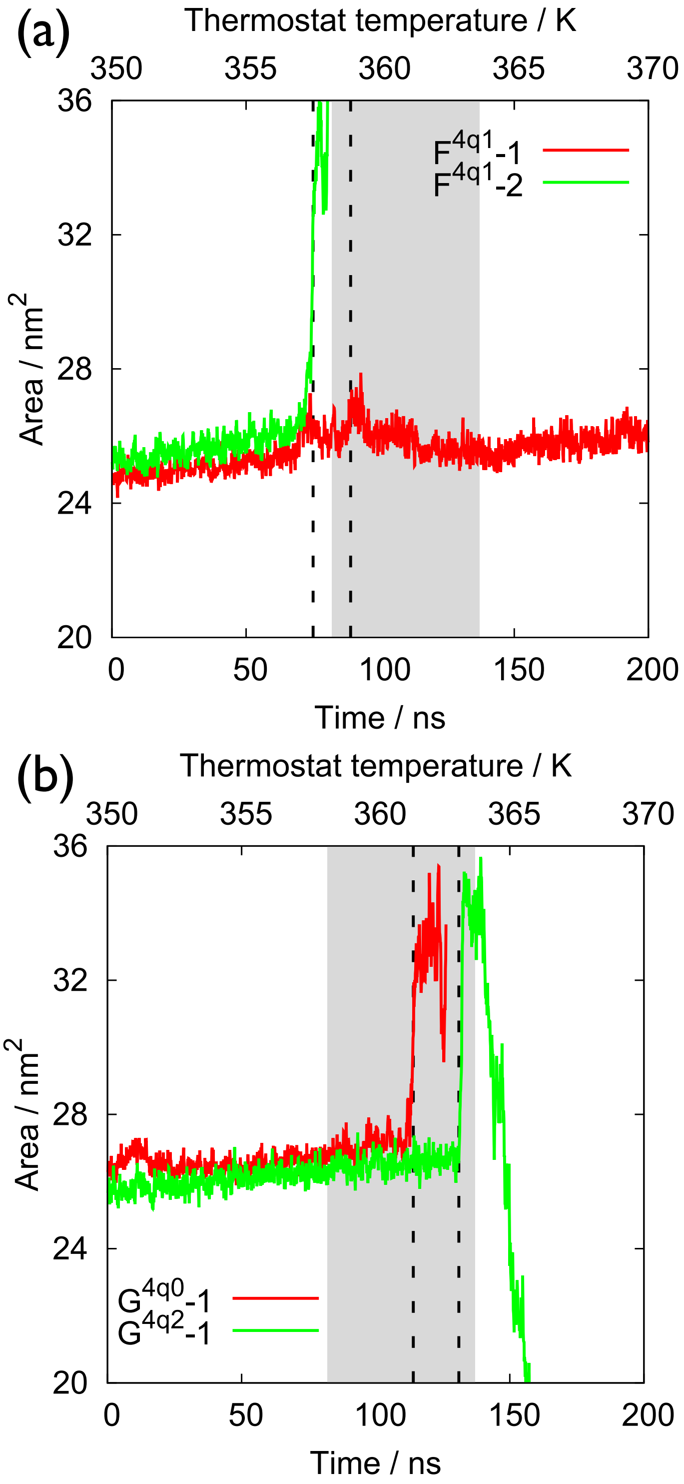

Fig. S11 The area of the bilayer as a function of time/temperature for (a) F^{4q1}-1 and F^{4q1}-2 and (b) G^{4q0}-1 and G^{4q2}-1 heating simulations. The vertical dashed lines indicate the transition temperature of each run. The shaded indicates the temperature range for the phase transition of for phase transition of mixed TS:SDBS bilayers, ratio 3:1, in the absence of NDs.

References

1 A. S. Barnard and M. Sternberg, *J. Mater. Chem.*, 2007, **17**, 4811–4819.

2 M. Elstner, D. Porezag, G. Jungnickel, J. Elsner, M. Haugk, T. Frauenheim, S. Suhai and G. Seifert, *Phys. Rev. B*, 1998, **58**, 7260.

3 B. Aradi, B. Hourahine and T. Frauenheim, *J. Phys. Chem. A*, 2007, **111**, 5678–5684.

4 A. D. Becke, *Phys. Rev. B*, 1993, **98**, 5648–5652.

5 C. Lee, W. Yang and R. Parr, *Phys. Rev., B*, 1988, **37**, 785–789.

6 M. J. Frisch, G. W. Trucks, H. B. Schlegel, G. E. Scuseria, M. A. Robb, J. R. Cheeseman, J. T. V. J. A. Montgomery, K. N. Kudin, J. C. Burant, J. M. Millam, S. S. Iyengar, J. Tomasi, V. Barone, B. Mennucci, M. Cossi, G. Scalmani, N. Rega, G. A. Petersson, H. Nakatsuji, M. Hada, M. Ehara, K. Toyota, R. Fukuda, J. Hasegawa, M. Ishida, T. Nakajima, Y. Honda, O. Kitao, H. Nakai, M. Klene, X. Li, J. E. Knox, H. P. Hratchian, J. B. Cross, C. Adamo, J. Jaramillo, R. Gomperts, R. E. Stratman, O. Yazyev, A. J. Austin, R. Cammi, C. Pomelli, J. W. Ochterski, P. Y. Ayala, K. Morokuma, G. A. Voth, P. Salvador, J. J. Dannenberg, V. G. Zakrzewski, S. Dapprich, A. D. Daniels, M. C. Strain, O. Farkas, D. K. Malick, A. D. Rabuck, K. Raghavachari, J. B. Foresman, J. V. Ortiz, Q. Cui, A. G. Baboul, S. Clifford, J. Cioslowski, B. B. Stefanov, G. Liu, A. Liashenko, P. Piskorz, I. Komaromi, R. L. Martin, D. J. Fox, T. Keith, M. A. Al-Laham, C. Y. Peng, A. Nanayakkara, M. Challacombe, P. M. W. Gill, B. Johnson, W. Chen, M. W. Wong, C. Gonzalez and J. A. Pople, *Gaussian, Inc., Pittsburgh PA*.

7 A. E. Reed, R. B. Weinstock and F. Weinhold, *J. Chem. Phys.*, 1985, **83**, 735–746.

8 R. W. Pastor and A. D. MacKerell, Jr, *J. Phys. Chem. Lett.*, 2011, **2**, 1526–1532.